Effects of a Preembedded Axial Magnetic Field on the Current Distribution in a Z-Pinch Implosion

D. Mikitchuk,[1,*] M. Cvejić,[1] R. Doron,[1] E. Kroupp,[1] C. Stollberg,[1] Y. Maron,[1] A. L. Velikovich,[2] N. D. Ouart,[2] J. L. Giuliani,[2] T. A. Mehlhorn,[2] E. P. Yu,[3] and A. Fruchtman[4]

[1]*Weizmann Institute of Science, Rehovot 76100, Israel*

[2]*Plasma Physics Division, Naval Research Laboratory, Washington, DC 20375, USA*

[3]*Sandia National Laboratories, P.O. Box 5800, Albuquerque, New Mexico 87185-1186, USA*

[4]*Holon Institute of Technology, P.O. Box 305, Holon 58102, Israel*

(Received 2 May 2018; revised manuscript received 8 November 2018; published 30 January 2019)

The fundamental physics of the magnetic field distribution in a plasma implosion with a preembedded magnetic field is investigated within a gas-puff Z pinch. Time and space resolved spectroscopy of the polarized Zeeman effect, applied for the first time, reveals the impact of a preembedded axial field on the evolution of the current distribution driven by a pulsed-power generator. The measurements show that the azimuthal magnetic field in the imploding plasma, even in the presence of a weak axial magnetic field, is substantially smaller than expected from the ratio of the driving current to the plasma radius. Much of the current flows at large radii through a slowly imploding, low-density plasma. Previously unpredicted observations in higher-power imploding-magnetized-plasma experiments, including recent, unexplained structures observed in the magnetized liner inertial fusion experiment, may be explained by the present discovery. The development of a force-free current configuration is suggested to explain this phenomenon.

DOI: 10.1103/PhysRevLett.122.045001

Compression of magnetic flux and magnetized plasma is a fundamental problem manifested in a variety of conducting fluid phenomena in laboratory plasmas and astrophysics [1–5]. Recently, this subject has gained particular interest due to the advances in producing plasmas of high temperature and density for fusion purposes, based on the approach of magnetized plasma compression [3,6]. These advances follow three decades of experimental [7–14] and theoretical [15,16] research. Some of the magnetized-plasma implosion experiments [7,8,11,17–19] reveal new and unpredicted phenomena, yet to be fully understood, which dramatically differ from those observed in implosion experiments without a preembedded axial magnetic field. These include significant changes in the plasma dynamics and radiation emission properties, specifically, (i) the formation of helical structures [17,18], (ii) larger than predicted implosion time and plasma radius at stagnation [18,19] accompanied by strong mitigation of instabilities [11,18], and (iii) reduction of the continuum [7,8] and K-shell emission [11]. In order to advance the concept of magnetized plasma compression, it is essential to understand the governing mechanisms of these phenomena.

A key parameter for the understanding of the physics occurring during the implosion and at stagnation is the compressing azimuthal magnetic field (B_θ). Knowledge of the magnetic field is required for inferring the current distribution, the magnetic field diffusion, the energy balance, and for comparisons with simulations. However, reliable experimental data on the B-field distribution in Z pinches are scarce due to the high electron densities, high ion velocities, and transient nature of the plasma, which make measurements of B fields in such plasmas rather difficult. We note a few examples of such spectroscopic measurements in gas-puff Z pinches [20–22], and measurements based on Faraday rotation in wire-array Z pinches [23].

Here, we present an experimental determination of B_θ throughout the magnetized plasma implosion, achieved using a noninvasive spectroscopic technique that provides a high sensitivity for the Zeeman effect [24]. This technique is based on the polarization properties of the Zeeman components for light emission viewed parallel to the B field, as described in Refs. [25–28], and recently implemented for Z-pinch implosions [22]. These measurements showed that the application of an initial axial magnetic field (B_{z0}) has a significant effect on the current distribution in the plasma: a large part of the current does not flow in the imploding plasma, rather it flows through a low-density plasma (LDP) residing at large radii (here, by "current distribution" we mean the partition of the total current between the flow in the imploding plasma and the LDP). We believe that these findings are of general nature and can explain various unexplained phenomena mentioned above.

We note that previous measurements in classical Z pinches have indicated that during the stagnation some of the current is carried by an imploding trailing plasma [23,29].

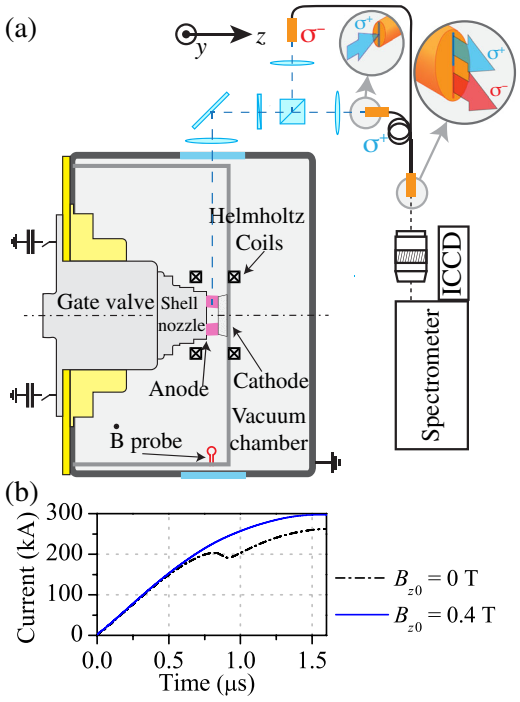

FIG. 1. (a) Schematic description of the experimental setup and spectroscopic system used for B_θ measurements. (b) Shot-averaged current traces obtained with a B-dot probe ($z = 5$ mm, $r = 120$ mm) for different values of B_{z0} (more details are given in the Supplemental Material [30]).

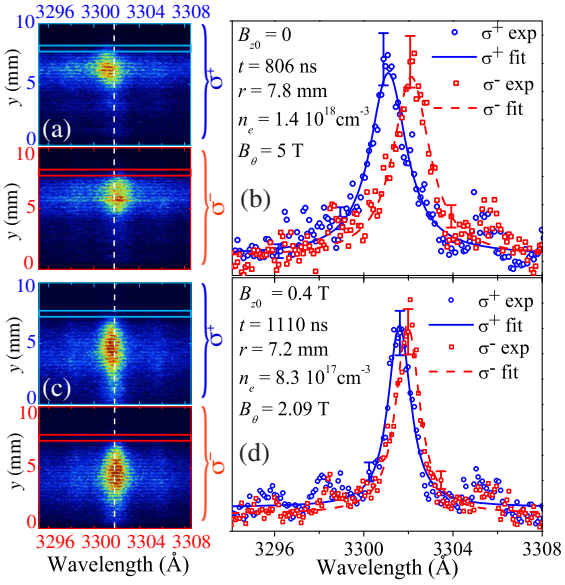

FIG. 2. (a) Spectral image of the Ar III $4s - 4p$ transition ($\lambda = 3301.85$ Å), for $B_{z0} = 0$. (b) Spectral line shapes of the σ^+ (blue circles) and σ^- (red squares) Zeeman components along with the best fits (blue solid and red dashed lines). (c) Spectral image for $B_{z0} = 0.4$ T. (d) Explanations are the same as in (b). y is the distance of the chord to the axis. The dashed white vertical line in (a) and (c) represents the unshifted position of the line center ($B_\theta = 0$). The horizontal lines mark the lineout positions.

However, here we show a completely different phenomenon that is directly related to the presence of an applied B_z.

In our configuration [Fig. 1(a)], a cylindrical argon gas-puff shell (initial radius 19 mm and mass 30 μg/cm, as determined by interferometry), containing a preembedded, quasistatic axial magnetic flux ($B_{z0} \leq 0.4$ T), prefills the anode-cathode gap (10 mm). Subsequently, a pulsed current (rising to 300 kA in 1.6 μs) is driven through the gas, ionizes it, and generates an azimuthal magnetic field that compresses the plasma radially inward together with the embedded B_z field. B_{z0} is generated by a pair of Helmholtz coils (HC) carrying a long current pulse (~5 ms) to allow for the diffusion of B_{z0} into the anode-cathode gap.

As shown in Fig. 1(a), the imploding plasma column is radially observed. The collected light passes through a quarter-wave plate that transforms the circularly polarized σ^+ and σ^- components into orthogonal linear polarizations that are subsequently split using a polarizing beam splitter. Each of the two polarizations is then imaged on a separate linear array of 50 optical fibers. The two ends of the fiber arrays are imaged along the entrance slit of a high-resolution (0.3 Å), imaging spectrometer; its output coupled to a gated (10 ns) intensified charge-coupled device (ICCD). This setup allows for a simultaneous recording of the two polarization components, emitted from exactly the same plasma volume, on different parts of a single detector, with a spatial resolution of 0.3 mm in the radial and axial directions.

Here, for the determination of B_θ, we use the σ^+ and σ^- Zeeman components of the Ar III $(^4S)4s\,^5S_2 - (^4S)4p\,^5P_2$ transition ($\lambda = 3301.85$ Å). Figure 2(a) presents a typical spectral image obtained at $z = 5$ mm ($z = 0$ is the anode surface) and $t = 806$ ns ($t = 0$ is the beginning of the current pulse) for $B_{z0} = 0$. The upper and lower halves show the plasma emission of the σ^+ and σ^- components, respectively, chordally integrated along the line of sight. Figure 2(b) shows the line shapes of the σ^+ and σ^- Zeeman components, obtained from the spectral image [Fig. 2(a)] by integrating the data over $\Delta y = 0.3$ mm at the outermost y of the plasma, along with their best fits. r_{imp} is defined at 20% of the peak emission after inverse Abel transform of the Ar III line intensity distribution (the Ar III line is optically thin and 2D images confirm that the plasma posses cylindrical symmetry). For $\vec{B} = B_\theta\hat{\theta}$, using the emission from the outermost plasma radii ensures that the line of sight is parallel to $\vec{B}$. It was verified, using visible 2D imaging, that the outermost radii of the imploding plasma and of the Ar III emission coincide.

Since the Zeeman splitting within each of the σ components is small ($\leq$0.025 Å for $B = 1$ T), each of the σ^+ and σ^- line shapes is fitted with a Voigt profile, where the Gaussian part accounts for instrumental and Doppler broadening, and the Lorentzian part is due to the Stark broadening. B_θ is then extracted from the wavelength difference between the peaks ($\Delta\lambda$) of the best fits [where

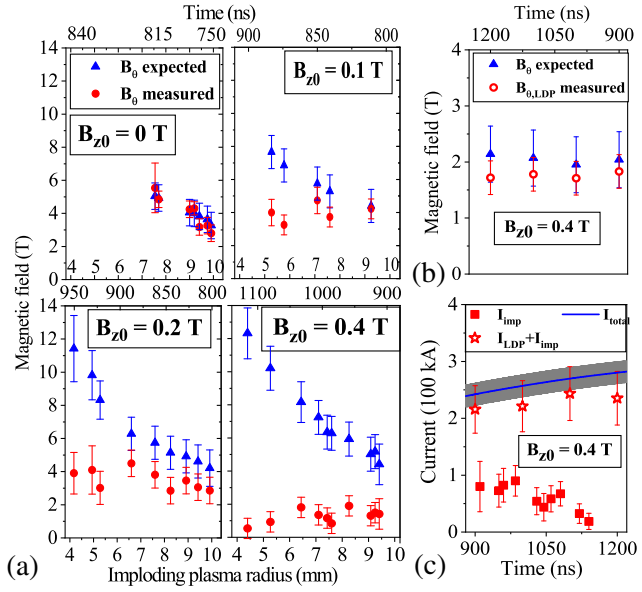

FIG. 3. (a) B_θ as a function of the outer imploding plasma radius, measured at $z = 3.5$ mm for $B_{z0} = 0$, 0.1, 0.2, and 0.4 T, together with the B_θ expected, calculated using the total current. The upper scale shows the typical times that correspond to each plasma radius (times of stagnation for $B_{z0} = 0$, 0.1, 0.2, and 0.4 T are 860 ± 20, 920 ± 20, 1030 ± 30, and 1160 ± 40 ns, respectively). (b) B_θ measured and B_θ expected as a function of time at the LDP outer radius ($r_{\mathrm{out,LDP}} \sim 25$–27 mm) at $z = 3.5$ mm for $B_{z0} = 0.4$ T. (c) Currents inferred from B_θ measurements within the imploding plasma (red squares), I_{imp}, and within the LDP outer radius (red stars), $I_{\mathrm{LDP}} + I_{\mathrm{imp}}$, together with I_{total} (blue line) from the B-dot measurement, for $B_{z0} = 0.4$ T. Grey region around the I_{total} represents uncertainty in the total current measurement.

$B_\theta(\mathrm{T}) = 5 \times \Delta\lambda(\text{Å})$ [24], for the Ar III line], and n_e is obtained from the Lorentzian width.

Figures 2(c) and 2(d) are the same as Figs. 2(a) and 2(b) but for $B_{z0} = 0.4$ T, obtained at $t = 1110$ ns. The spectral images in Fig. 2 are chosen such that, at the time of their recording, the outer plasma radius is similar ($r_{\mathrm{imp}} \approx 7.8$ mm for $B_{z0} = 0$, and $r_{\mathrm{imp}} \approx 7.2$ mm for $B_{z0} = 0.4$ T). For these conditions, and assuming the entire current is flowing through the imploding plasma, we expect that B_θ would be lower for the case of $B_{z0} = 0$, due to the significantly smaller current measured by the B-dot probe at the time of the spectra recording [~195 kA for $B_{z0} = 0$, ~270 kA for $B_{z0} = 0.4$ T, as seen from Fig. 1(b)]. However, while the measured B_θ in the case of $B_{z0} = 0$ is $B_\theta \cong 5$ T, as expected, in the case of $B_{z0} = 0.4$ T, the measured $B_\theta \cong 2.1$ T is much lower than expected from Ampere's law. Considering the fact that, in implosions with axial B field, the total $\vec{B}$ might be not parallel to our line of sight, the calculations show that the true B_θ is even lower than 2.1 T.

Figure 3(a) shows the measurements of B_θ at the plasma outer radius for $B_{z0} = 0$, 0.1, 0.2, and 0.4 T, together with B_θ expected, calculated by assuming the entire measured circuit current flows within the plasma radius ($B_\theta = \mu_0 I/2\pi r_{\mathrm{imp}}$). We note that each data point is obtained from a separate shot, and that different sets of shots have shown that the results were reproducible to within the error bars indicated. For $B_{z0} = 0$, B_θ measured shows that the entire current flows within the imploding shell. On the other hand, for $B_{z0} > 0$, B_θ measured differs significantly from B_θ expected. This phenomenon is observed over the entire anode-cathode gap (see Supplemental Material [30]). This shows that the application of B_z significantly affects the current distribution in the plasma, such that only part of the current flows through the imploding plasma. Furthermore, it is seen that the fraction of the total current that flows in the imploding plasma decreases with B_{z0}. Additionally, Fig. 3(c) shows that for $B_{z0} = 0.4$ T the current within the imploding plasma drops with time. Before we discuss the implications of these measurements on the plasma dynamics, we first show that the missing current flows in a low-density plasma (LDP) residing at radii larger than that of the imploding plasma.

To this end, plasmas were searched for up to the vacuum chamber wall using 2D and spectral imaging (see Supplemental Material [30]). These measurements revealed the existence of plasma at $20 \lesssim r \lesssim 27$ mm, which consists of argon, carbon, and hydrogen ions ($10^{16} \lesssim n_e \lesssim 10^{17}\,\mathrm{cm}^{-3}$ from Stark broadening, $T_e \sim 4$–6.5 eV from line intensities). B_θ measurements at the outer radius of this LDP, using Zeeman splitting of the C IV $3s - 3p$ transition ($\lambda = 5801$ Å) are presented in Fig. 3(b). It shows that the current flowing within $\lesssim 27$ mm accounts for nearly the entire current measured by the B dot [see Fig. 3(c)], providing a definite answer for the missing current in the imploding plasma.

It is emphasized that the LDP is also observed when $B_{z0} = 0$. However, its n_e and T_e remain low throughout the implosion ($n_e \lesssim 10^{16}$ cm^{-3}, $T_e \leq 2$ eV), consistent with the absence of current flow there. It is only in the presence of $B_{z0} > 0$ that the LDP carries a significant part of the current.

It can be further seen in Fig. 3 that the ratio of I_{LDP} to the imploding plasma current rises with time. This is explained by the rise of the imploding plasma impedance due to the increase of $d(LI)/dt$ and resistance (plasma cross section is decreasing, but its resistivity, inferred from T_e measurements, is nearly constant), whereas the LDP impedance remains almost constant [this explains the difference between the current traces shown in Fig. 1(b)]. We note that I_{LDP} may be also limited by ion acoustic turbulence (IAT) [31], which for the LDP parameters limits I_{LDP} to ~100–200 kA.

The present measurements demonstrate that, in the presence of B_z, much of the current flows at large radii in a slowly imploding, low-density plasma. Here, we show that these findings can explain the unpredicted and unexplained phenomena observed in previous studies of B_z compression [7–9,11,17–19,32,33]. For example: (i) B_z

significantly slows down the plasma implosion and increases the final stagnation radius [18,19], while simulations using the NRL 1D radiation-MHD code [34] predict that the B_z counterpressure is too low to have such significant impact on the plasma dynamics. In our experiment, the implosion time for $B_{z0} = 0.4$ T is ~35% longer than for $B_{z0} = 0$, while simulations, assuming the entire current flows in the imploding plasma, predict an implosion longer by only ~2%. (ii) A very small $B_{z0} = 0.28$ T relative to the B_θ generated by the discharge current, practically eliminates the x-ray yield in the experiment on the 2.5-MA GIT-12 generator [11]. (iii) A relative very small $B_{z0} =$ 0.1–0.2 T significantly stabilizes the implosion and stagnation in our experiment [18], and in the experiments on the 0.9-MA COBRA [32] and 1-MA ZEBRA facilities [33]. (iv) Unexpectedly large pitch angle of the helix-like plasma structures is observed in the magnetized liner inertial fusion experiments [17]. Assuming the observed plasma structure is generated at the outer radius of the imploding plasma and is along $\vec{B}$, a very small pitch angle is expected since $B_\theta \gg B_{z0}$. We suggest that the large pitch angle is induced by two processes: the reduced fraction of discharge current that flows in the imploding plasma, and an amplification of B_z due to an azimuthal current density (j_θ) in the LDP (that might be present outside the liner due to liner evaporation or plasma from electrodes), as explained below. We note that the possibility of current flow in peripheral plasma of the magnetized liner inertial fusion experiment has been already suggested [35], together with a mechanism, that is different from the one outlined here, to explain the large pitch angle.

The properties of the peripheral plasmas, which might have shunted current from the imploding plasma, are not known in the experiments mentioned above, nor known is the fraction of the current flow outside this plasma. The present Letter demonstrates that such Zeeman-effect measurements might be essential for revealing small fractions (~10%) of current loss to the LDP, while they cannot be inferred from the plasma implosion time (as commonly done), although such current losses can significantly affect the final stagnating plasma properties.

We suggest a possible explanation of this phenomenon. It is known [36] that plasma in constant and uniform electric ($\vec{E}$) and magnetic ($\vec{B}$) fields, which are perpendicular (i.e., $B_{z0} = 0$), reaches the drift velocity $\vec{v}_{\rm drift} = (\vec{E} \times \vec{B})/B^2$. At this velocity, the effective electric field $\vec{E}_{\rm eff} = \vec{E} + \vec{v} \times \vec{B}$ vanishes, and j_z is driven only by spatial gradients of the plasma parameters. For $B_{z0} = 0$, the current in the LDP due to the gradients in the plasma properties is very small and the entire current can flow in the imploding plasma. This situation changes when $B_{z0} > 0$, since at $v_{\rm drift}$, $\vec{E}_{\rm eff} \neq 0$, allowing current flow in the LDP. This can be seen from the generalized Ohm's law for constant $\vec{E} = E_z\hat{z}$, and $\vec{B} = B_\theta\hat{\theta} + B_z\hat{z}$:

$$\frac{\partial \vec{j}}{\partial t} = \frac{\nu_{\rm ei}}{\eta}(\vec{E} + \vec{v} \times \vec{B}) - \nu_{\rm ei}\vec{j} - \omega_{\rm ce}\frac{\vec{j} \times \vec{B}}{|\vec{B}|}, \qquad (1)$$

where $\vec{v}$ is the plasma velocity, its evolution is given by $\partial\vec{v}/\partial t = \vec{j} \times \vec{B}/\rho$ ($\nu_{\rm ei}$ as electron-ion collision frequency, $\omega_{\rm ce}$ as electron cyclotron frequency, and η as plasma resistivity). The pressure terms are omitted since, for the LDP conditions, $\beta \sim 10^{-2}$–10^{-1}. The steady-state solution of Eq. (1) is the force-free current configuration, $j_z = (E_z/\eta)(B_z/B)^2$, $j_\theta = (E_z/\eta)B_zB_\theta/B^2$, and $v_r = v_{\rm drift}$, which for the LDP parameters is reached on timescales [36] of $\tau_{\rm steady} = \nu_{\rm ei}/(\omega_{\rm ce}\omega_{\rm ci}) \sim$ 10–30 ns ($\omega_{\rm ci}$ is ion cyclotron frequency) that is much shorter than the characteristic implosion time (hundreds ns). Note that j_θ in the LDP generates an additional B_z flux in the LDP and in the imploding plasma.

While the LDP plasma carries a large fraction of the current, no significant inward motion of this plasma is observed. Indeed, by estimating the $v_{\rm drift}$ of the LDP for $E_{\rm z,LDP} \sim 1.5 \times 10^4$ V/m (using Spitzer resistivity and assuming uniform current distribution for $I_{\rm z,LDP} \sim 200$ kA and $20 \leq r_{\rm LDP} \leq 27$ mm) and $B_z \sim B_\theta \sim 1$ T, yields $v_{\rm drift} \sim 7.5 \times 10^5$ cm/s that is small compared to the imploding plasma velocity, $v_{\rm imp} \approx 3 \times 10^6$ cm/s. This discussion does not apply for the imploding plasma since the assumptions of constant $\vec{E}$ and $\vec{B}$ ($\tau_{\rm steady} \sim t_{\rm implosion} \sim 1$ μs) and the neglect of the pressure terms are not valid there.

We emphasize that the development of the force-free configuration in LDP is suggested here only as a possibility. To test this explanation requires further measurements, in particular investigation of a B_z increase due to possible j_θ in the LDP. In addition, three-dimensional modeling that involves processes beyond MHD is required to explain the observed phenomena and to test our hypothesis. Simulations of this kind have been recently published [37,38].

As said above, the significant effects of B_{z0} on the implosion dynamics are due to current loss to the LDP, and thus occur at B_{z0} values much lower than required for affecting the implosion dynamics, based on the compressed-B_z-pressure considerations. The values of B_{z0} (relative to B_θ) in the various experiments that affect significantly the implosion dynamics require further investigations; it depends on the geometry, the resistivity of the imploding plasma and the LDP, and on the LDP properties relevant to IAT or to the force-free current timescale. For example, in our experiment, it was found that ~10× reduction of the LDP density, obtained by moving the Helmholtz coils outside of the vacuum chamber, together with a few initial discharges to clean the electrodes from adsorbates, almost eliminated the current conduction through the LDP for B_{z0} up to 0.3 T, also consistent with IAT estimates. The present results demonstrate that a LDP, which may inevitably be present in high-power systems due to various processes, can affect severely the current

distribution, and possibly lead to the development of force-free configurations.

Invaluable discussions with S. Slutz, U. Shumlak, M. Cuneo, D. Sinars, G. Rochau, N. Fisch, D. A. Hammer, H. R. Strauss, A. Fisher, and M. Herrmann are gratefully acknowledged. This work was supported in part by the Cornell Multi-University Center for High Energy-Density Science (USA), the Bi-National Israel-USA Science Foundation, the Office of Naval Research (USA), and the Israel Scientific Foundation.

D. M. and M. C. contributed equally to this work.

*Corresponding author.
Dimitry.Mikitchuk@weizmann.ac.il

[1] T. A. Mehlhorn, IEEE Trans. Plasma Sci. **42**, 1088 (2014).
[2] J. L. Giuliani and R. J. Commisso, IEEE Trans. Plasma Sci. **43**, 2385 (2015).
[3] M. R. Gomez *et al.*, Phys. Rev. Lett. **113**, 155003 (2014).
[4] O. V. Gotchev, P. Y. Chang, J. P. Knauer, D. D. Meyerhofer, O. Polomarov, J. Frenje, C. K. Li, M. J.-E. Manuel, R. D. Petrasso, J. R. Rygg, F. H. Séguin, and R. Betti, Phys. Rev. Lett. **103**, 215004 (2009).
[5] J. O. Stenflo, Astron. Astrophys. **517**, A37 (2010).
[6] S. A. Slutz, M. C. Herrmann, R. A. Vesey, A. B. Sefkow, D. B. Sinars, D. C. Rovang, K. J. Peterson, and M. E. Cuneo, Phys. Plasmas **17**, 056303 (2010).
[7] F. S. Felber, F. J. Wessel, N. C. Wild, H. U. Rahman, A. Fisher, C. M. Fowler, M. A. Liberman, and A. L. Velikovich, J. Appl. Phys. **64**, 3831 (1988).
[8] F. S. Felber, M. M. Malley, F. J. Wessel, M. K. Matzen, M. A. Palmer, R. B. Spielman, M. A. Liberman, and A. L. Velikovich, Phys. Fluids **31**, 2053 (1988).
[9] R. K. Appartaim and A. E. Dangor, J. Appl. Phys. **84**, 4170 (1998).
[10] G. G. Zukakishvili, K. N. Mitrofanov, E. V. Grabovskii, and G. M. Oleinik, Plasma Phys. Rep. **31**, 652 (2005).
[11] A. V. Shishlov, R. B. Baksht, S. A. Chaikovsky, A. V. Fedunin, F. I. Fursov, V. A. Kokshenev, N. E. Kurmaev, A. Yu. Labetsky, V. I. Oreshkin, N. A. Ratakhin, A. G. Russkikh, and S. V. Shlykhtun, Laser Phys. **16**, 183 (2006).
[12] J. P. Knauer, O. V. Gotchev, P. Y. Chang, D. D. Meyerhofer, O. Polomarov, R. Betti, J. A. Frenje, C. K. Li, M. J.-E. Manuel, R. D. Petrasso, J. R. Rygg, and F. H. Séguin, Phys. Plasmas **17**, 056318 (2010).
[13] P. Y. Chang, G. Fiksel, M. Hohenberger, J. P. Knauer, R. Betti, F. J. Marshall, D. D. Meyerhofer, F. H. Séguin, and R. D. Petrasso, Phys. Rev. Lett. **107**, 035006 (2011).
[14] M. Hohenberger, P.-Y. Chang, G. Fiksel, J. P. Knauer, R. Betti, F. J. Marshall, D. D. Meyerhofer, F. H. Séguin, and R. D. Petrasso, Phys. Plasmas **19**, 056306 (2012).
[15] F. S. Felber, M. A. Liberman, and A. L. Velikovich, Phys. Fluids **31**, 3675 (1988).
[16] F. S. Felber, M. A. Liberman, and A. L. Velikovich, Phys. Fluids **31**, 3683 (1988).
[17] T. J. Awe *et al.*, Phys. Rev. Lett. **111**, 235005 (2013).
[18] D. Mikitchuk, C. Stollberg, R. Doron, E. Kroupp, Y. Maron, H. R. Strauss, A. L. Velikovich, and J. L. Giuliani, Trans. Plasma Sci. **42**, 2524 (2014).
[19] A. G. Rousskikh, A. S. Zhigalin, V. I. Oreshkin, V. Frolova, A. L. Velikovich, G. Yu. Yushkov, and R. B. Baksht, Phys. Plasmas **23**, 063502 (2016).
[20] G. Davara, L. Gregorian, E. Kroupp, and Y. Maron, Phys. Plasmas **5**, 1068 (1998).
[21] R. P. Golingo, U. Shumlak, and J. Den Hartog, Rev. Sci. Instrum. **81**, 126104 (2010).
[22] G. Rosenzweig, E. Kroupp, A. Fisher, and Y. Maron, J. Instrum. **12**, P09004 (2017).
[23] V. V. Ivanov, A. A. Anderson, D. Papp, A. L. Astanovitskiy, V. Nalajala, and O. Dmitriev, Phys. Plasmas **22**, 092710 (2015).
[24] R. Doron, D. Mikitchuk, C. Stollberg, G. Rosenzweig, E. Stambulchik, E. Kroupp, Y. Maron, and D. A. Hammer, High Energy Density Phys. **10**, 56 (2014).
[25] F. C. Jahoda, F. L. Ribe, and G. A. Sawyer, Phys. Rev. **131**, 24 (1963).
[26] N. J. Peacock and B. A. Norton, Phys. Rev. A **11**, 2142 (1975).
[27] J. F. Seely, U. Feldman, N. R. Sheeley, Jr., S. Suckewer, and A. M. Title, Rev. Sci. Instrum. **56**, 855 (1985).
[28] T. Shikama and P. M. Bellan, Rev. Sci. Instrum. **84**, 023507 (2013).
[29] Y. Maron, A. Starobinets, V. I. Fisher, E. Kroupp, D. Osin, A. Fisher, C. Deeney, C. A. Coverdale, P. D. Lepell, E. P. Yu, C. Jennings, M. E. Cuneo, M. C. Herrmann, J. L. Porter, T. A. Mehlhorn, and J. P. Apruzese, Phys. Rev. Lett. **111**, 035001 (2013).
[30] See Supplemental Material at http://link.aps.org/supplemental/10.1103/PhysRevLett.122.045001 contains: 1) Azimuthal magnetic field measurements at different z-positions, 2) measurements of the low-density plasma properties, 3) measurements of the evolution of the initial axial magnetic field at different radial positions, and 4) measurements of the discharge current evolution for shots with and without axial magnetic field.
[31] D. D. Ryutov, M. S. Derzon, and M. K. Matzen, Rev. Mod. Phys. **72**, 167 (2000).
[32] N. Qi, P. de Grouchy, P. C. Schrafel, L. Atoyan, W. M. Potter, A. D. Cahill, P.-A. Gourdain, J. B. Greenly, D. A. Hammer, C. L. Hoyt, B. R. Kusse, S. A. Pikuz, and T. A. Shelkovenko, AIP Conf. Proc. **1639**, 51 (2014).
[33] F. Conti, J. Valenzuela, M. P. Ross, J. Narkis, F. Beg, H. Rahman, E. Ruskov, A. Anderson, and A. Covington, Int. Conf. Plasma Sci., 2018.
[34] J. Davis, J. L. Giuliani, Jr., and M. Mulbrandon, Phys. Plasmas **2**, 1766 (1995).
[35] D. D. Ryutov, T. J. Awe, S. B. Hansen, R. D. McBride, K. J. Peterson, D. B. Sinars, and S. A. Slutz, AIP Conf. Proc. **1639**, 63 (2014).
[36] L. Spitzer, *Physics of Fully Ionized Gases* (Courier Corporation, Mineola, New York, 2006).
[37] C. E. Seyler, M. R. Martin, and N. D. Hamlin, Phys. Plasmas **25**, 062711 (2018).
[38] A. B. Sefkow, Bull. Am. Phys. Soc. **61**, 2016.